IMMUNOHISTOLOGY

Cryosections from cell sheets were immunostained with monoclonal anti–keratin 3 antibodies (AE5, Progen Biotechnik), anti–β_1 integrin antibodies (P5D2, Santa Cruz Biotechnology), or anti-p63 antibodies (4A4, Santa Cruz Biotechnology) and fluorescein isothiocyanate–labeled or rhodamine-labeled secondary antibodies (Jackson ImmunoResearch Laboratories). Nuclei were costained with Hoechst 33342 (Molecular Probes) or propidium iodide (Sigma). Stained cells were observed using confocal laser scanning microscopy (LSM-510, Zeiss). The same concentration of corresponding normal nonspecific IgG provided negative controls, and native human corneal and limbal tissues were used as positive controls.

TRANSPLANTATION OF CELL SHEETS TO THE EYE

We removed the conjunctival and subconjunctival scar tissue from the cornea up to 3 mm outside the limbus to reexpose corneal stroma (Fig. 2, and a video clip in the Supplementary Appendix, available with the full text of this article at www.nejm.org). Subsequently, the harvested sheet of autologous oral mucosal epithelial cells was placed directly onto the exposed transparent stromal bed as described previously.[6,23] No sutures were required. The grafted corneal surface was then covered with a soft contact lens for protection during healing. After surgery, topical antibiotics (0.3 percent ofloxacin) and steroids (0.1 percent betamethasone) were initially applied four times a day and then tapered to three times a day. During the first week after surgery, betamethasone (1 mg per day) was administered orally to reduce postoperative inflammation. One month after surgery, the administration of topical corticosteroids was changed from 0.1 percent betamethasone to 0.1 percent fluorometholone. Because the patients had severe dry eye, proper wound healing could not be expected without tear supplementation. Preservative-free artificial tears were frequently used, and the puncta lacrimale of all the patients were occluded to increase tear retention.

RESULTS

CHARACTERIZATION OF TISSUE-ENGINEERED EPITHELIAL-CELL SHEETS

We compared cultured autologous oral mucosal-cell sheets with endogenous tissue both functionally and phenotypically. Oral mucosal epithelial cells cultured under these culture conditions resemble corneal epithelium, with three to five cell layers, small basal cells, flattened middle cells, and polygonal and flattened superficial cells (Fig. 1B), more than they resemble native oral mucosal epithelium (Fig. 1C), which is much thicker than corneal epithelium (Fig. 1D). The optical transparency of harvested cell sheets was equal to that of corneal epithelial-cell sheets originating from limbal stem cells (data not shown).[23]

Ultrastructural examination revealed an architecture of well-structured, compact, multilayered cell sheets with the expected microstructures of the native cells, including microvilli (Fig. 1E), tight junctions, desmosomes, and basement membrane. Such morphologic characteristics are similar to those of corneal epithelium in vivo. Native corneal epithelial cells and oral mucosal epithelial cells express keratin 3 as a characteristic phenotypic marker, and harvested epithelial-cell sheets also express keratin 3 (Fig. 1F).

The mean (±SE) colony-forming efficiency, calculated as the ratio of the number of stem or progenitor cells that can produce colonies to the total number of cells in the harvested tissue, was 2.1±0.9 percent for all four patients (with measurements performed in triplicate in each patient), confirming the presence of progenitor cells among the isolated oral mucosal epithelial cells. Correspondingly, β_1 integrin, reported to be an epithelial stem-cell and progenitor-cell marker[24] susceptible to digestion by trypsin, remained intact in the basal cells (Fig. 1G). The basal cells in the multilayered cell sheets also express p63 (Fig. 1H), a putative epithelial stem-cell marker.[25]

CLINICAL RESULTS OF TRANSPLANTATION OF THE CELL SHEET TO THE CORNEAL SURFACE

Attachment of the cell sheet to the stromal bed was spontaneous and uniform (Fig. 2, and video clip in the Supplementary Appendix). Within several minutes after placement without sutures, the grafted cell sheets remained intact and stably bound to the stromal surfaces, even after the extensive application of eyedrops. This observation is consistent with previous experiments with rabbit models, in which transplanted sheets of oral mucosal epithelial cells readily resisted outward displacement when the perimeters were pulled with forceps.

Immediately after surgery, the transplanted corneal surface was clear and smooth, without observable vascularization. Within one week, slit-lamp ex-

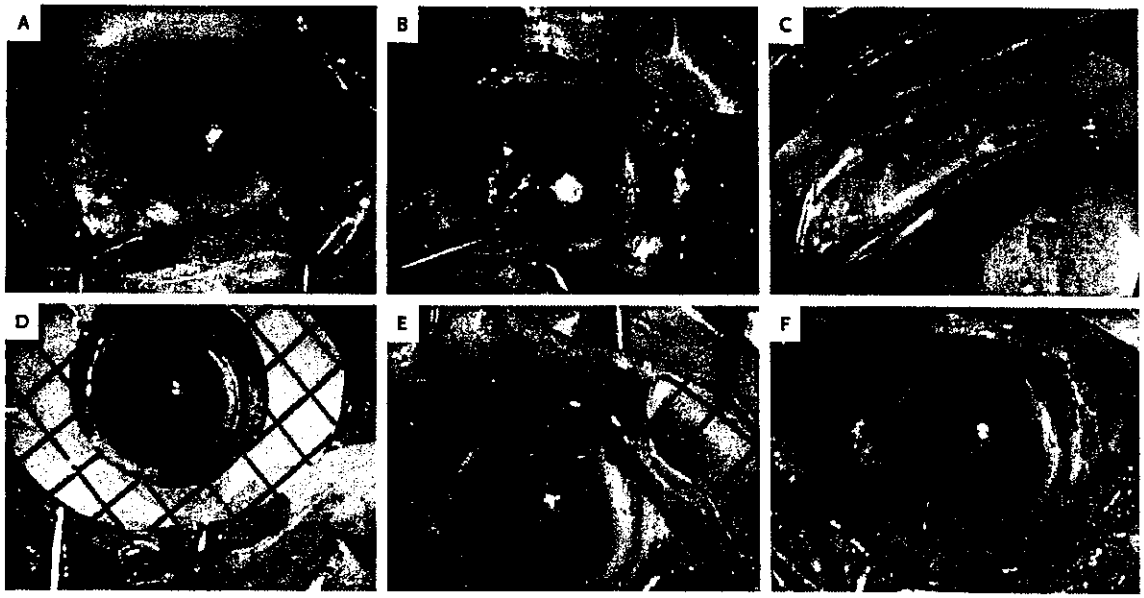

Figure 2. Transplantation Procedures for Tissue-Engineered Autologous Epithelial-Cell Sheets.

Preoperatively, the entire corneal surface was covered by conjunctival tissue with neovascularization (Panel A). In Panel B, conjunctival tissue over the cornea is surgically removed to reexpose transparent corneal stroma. Then, the sheet of tissue-engineered epithelial cells is harvested from a temperature-responsive culture insert with the use of a doughnut-shaped supporter ([black-and-white squares] Panel C) and placed on the stromal bed (Panel D). The sheet adheres to corneal stroma in a few minutes without sutures, and the supporter is removed (Panel E), leaving the cell sheet on the stroma (Panel F). A video clip can be viewed in the Supplementary Appendix, available with the full text of this article at www.nejm.org.

amination with fluorescein sodium staining showed complete reepithelialization of the corneal surface in all four eyes, revealing the tight junction-mediated barrier function. Corneal transparency was restored without any defects of the corneal epithelium. In all eyes, stromal vascularization gradually recurred in the peripheral cornea but not in the central zone. This vascularization was unlike subepithelial vascularization accompanied by conjunctival ingrowth, since it was localized to the deeper stroma and did not show the abnormally high fluorescein permeability characteristic of conjunctival epithelium.

During a mean follow-up period of 14 months, corneal transparency was maintained (Fig. 3 and Table 2). Maximally improved visual acuity was obtained 6, 2, 10, and 8 weeks after transplantation for Patients 1 through 4, respectively, and became stable thereafter. The length of time until visual acuity improved seemed to correspond to the length of time until the corneal stroma became less opaque. No complications were observed.

DISCUSSION

Our study shows that tissue-engineered cell sheets from autologous oral mucosal epithelium may serve as effective substitutes for allografts of limbal tissue in the reconstruction of the corneal and limbal surfaces. Four patients (four eyes) were consecutively treated with this approach, and corneal transparency was restored and postoperative visual acuity improved remarkably (Table 2). During the follow-up period, all corneal surfaces remained transparent, and there were no serious complications.

We developed this strategy on the basis of several observations from cell biology and medicine. First, in vivo oral mucosal epithelium expresses keratin 3, which is also expressed by the corneal epithelium but not by the epidermis.[1,27] Second, the excision of a small piece of oral mucosal tissue from the patient is straightforward, and the resulting wound heals within several days without incident or scarring. Third, transplantation of autologous

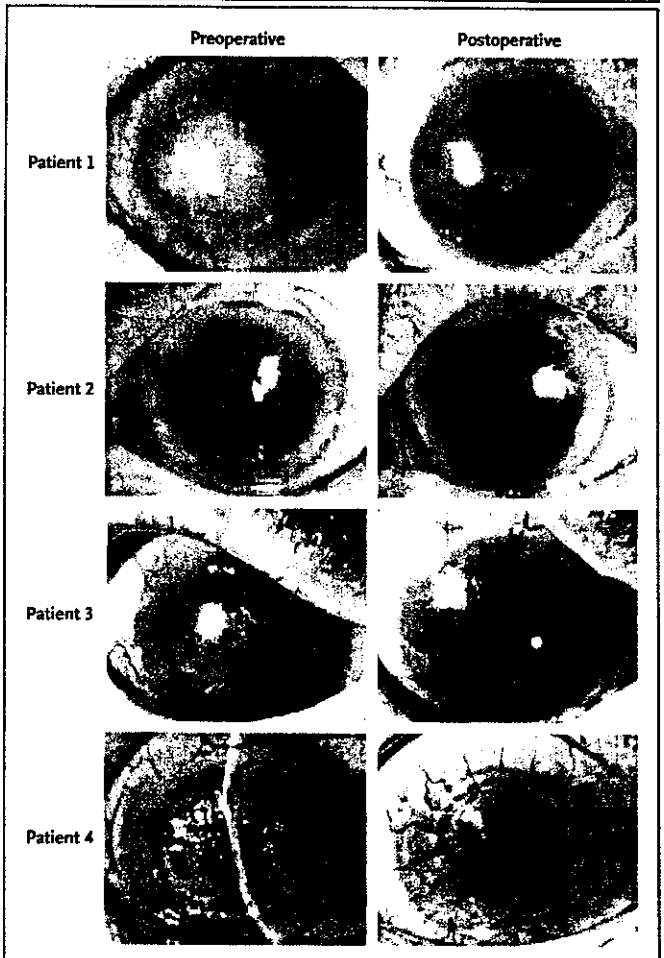

Figure 3. Eyes of Patients before and after Transplantation of Sheets of Tissue-Engineered Autologous Epithelial Cells.

These photographs were taken just before transplantation of the cell sheets and postoperatively at 13, 14, or 15 months.

buccal mucosal grafts directly onto ocular surfaces was previously reported in human patients[28] for the purposes of treating corneal ulcers, corneal perforations, and lid abnormalities (e.g., marginal entropion and trichiasis); these grafts are not useful for improving vision, since they contain opaque subepithelial fibrous tissue. In contrast, the transparency of carrier-free sheets of tissue-engineered epithelial cells fabricated from oral mucosal epithelial cells is similar to the transparency of corneal epithelial-cell sheets originating from limbal stem cells.[23]

Reconstruction with autologous oral mucosal epithelial cells offers substantial clinical advantages over allogeneic transplantation for treating severe diseases such as the Stevens–Johnson syndrome and ocular pemphigoid. It averts the risks of allogeneic immunorejection and immunosuppression. Severe tear-film and lid abnormalities often associated with these diseases continue to be a challenge, since immunologically driven inflammation of the ocular surface persists chronically in these patients.

Although decisive epithelial stem-cell markers that could provide evidence of the presence of these stem cells in grafted cell sheets have not yet been established,[29] results from colony-forming assays for oral mucosal epithelium show that excised oral tissue contains epithelial stem cells or at least progenitor cells. Since ocular surfaces that have been grafted with cell sheets retain their transparency for more than one year, and because the life spans of transient amplifying cells (cells committed to epithelial differentiation) are believed to be less than one year,[30] we conclude that progenitor cells with the potential to differentiate into new corneal epithelial phenotype are present in autografts of cell sheets.

Conjunctival epithelial cells invade the cornea after allogeneic transplantation because of the gradual depletion of allogeneic corneal epithelial cells due to epithelial rejection or stem-cell depletion.[31-33] It is unknown whether this also applies to autologous transplants. In the four eyes we studied, limited stromal vascularization occurred within a few months after transplantation of the cell sheet and reached a stable state within six months, with no appreciable growth thereafter. This stromal vascularization was observed only beneath cell sheets on peripheral corneas and should be distinguished from the subepithelial neovascularization accompanied by conjunctival ingrowth that results from the stem-cell loss associated with allografts, which occurs several months after transplantation. This finding suggests that grafted oral mucosal epithelial cells remained on the ocular surface.

It is possible that the reduction in host immunologic reactions associated with the grafting of autologous cells may minimize epithelial rejection, but further study is needed. The limited stromal neovascularization that we observed is probably caused by angiogenic factors secreted from tissue-engineered epithelial-cell sheets fabricated from oral mucosal epithelial cells originally located in

Table 2. Surgical Outcome in Four Patients Who Received Transplants of Tissue-Engineered Autologous Oral Mucosal-Cell Sheets.

Patient No.	Best Corrected Visual Acuity in Damaged Eye		Corneal Opacity (Grade)*			Complication	Months of Follow-up
	Preoperative†	Postoperative	Preoperative	1 Month after Surgery	At Last Observation		
1	Counting fingers	20/100	3	2	1	None	15
2	20/2000	20/25	3	1	1	None	14
3	Hand motion	20/300	3	1	1	None	14
4	20/2000	20/50	3	1	1	None	13

* The extent of corneal opacity was graded by three masked observers on the basis of the slit-lamp examination with a previously described system[26] and modifications for ocular-surface diseases. Grade 0 indicates clear or trace haze, grade 1 mild opacity, grade 2 moderately dense opacity partially obscuring details of the iris, and grade 3 severely dense opacity obscuring details of the intraocular structure. Grading is based on the opacity observed in all corneal layers, including epithelium, stroma, and endothelium.

† The visual acuity of patients who could not read a visual-acuity chart at a distance of 0.5 m was assessed by asking whether they could see the number of fingers held up by the examiner. If they could not, visual acuity was assessed by the patient's ability to see hand movement by the examiner.

vivo on the substantia propria, which is rich in vessels. However, the production of antiangiogenic factors such as thrombospondin by keratocytes[34] may limit vascularization to peripheral areas.

We observed that the transplanted cell sheets became more transparent and achieved smoother, integrated surfaces on the corneal stroma, further resembling normal corneal epithelium; a plateau was reached one to three months after transplantation. Originally, oral mucosal epithelium, located on substantia propria, is morphologically distinct from corneal epithelium in that it is much thicker and multilayered and has an irregular surface (Fig. 1C). The use of temperature-responsive harvesting allows the grafted carrier-free oral mucosal epithelial cells to interact immediately and directly with patients' corneal stromal keratocytes without interference from cell carriers such as fibrin gel and amniotic membranes.

Our transplantable epithelial-cell sheets used the common 3T3 feeder-layer method originally developed for the production of autologous epidermal-cell grafts[35] and used in the culture of other epithelial cells from various tissue sources, including the limbus.[16] This method has been clinically applied since the 1980s for the treatment of various skin conditions, including burns and giant nevi, although the Food and Drug Administration classifies these grafts as xenografts.

In summary, we have shown that sheets of tissue-engineered epithelial cells fabricated ex vivo from autologous oral mucosal epithelium are effective for reconstructing the ocular surface and restoring vision in patients with bilateral total stem-cell deficiencies. Long-term follow-up and experience with a large series of patients are needed to assess further the benefits and risks of this method, which offers the potential to treat severe ocular diseases that are resistant to standard approaches.

Supported by Grants-in-Aid for Scientific Research (15390530, 16200036, and 16300161), the High-Tech Research Center Program, and the Center of Excellence Program for the 21st Century from the Ministry of Education, Culture, Sports, Science, and Technology in Japan and by the Core Research for Evolution Science and Technology from the Japan Science and Technology Agency.

We are indebted to Professor David Grainger, Colorado State University, and Mr. Joseph Yang, Tokyo Women's Medical University, for their technical review.

REFERENCES

1. Schermer A, Galvin S, Sun TT. Differentiation-related expression of a major 64K corneal keratin in vivo and in culture suggests limbal location of corneal epithelial stem cells. J Cell Biol 1986;103:49-62.
2. Cotsarelis G, Cheng SZ, Dong G, Sun TT, Lavker RM. Existence of slow-cycling limbal epithelial basal cells that can be preferentially stimulated to proliferate: implications on epithelial stem cells. Cell 1989;57:201-9.
3. Thoft RA, Friend J. The X, Y, Z hypothesis of corneal epithelial maintenance. Invest Ophthalmol Vis Sci 1983;24:1442-3.
4. Buck RC. Measurement of centripetal migration of normal corneal epithelial cells in the mouse. Invest Ophthalmol Vis Sci 1985; 26:1296-9.
5. Tseng SC. Concept and application of limbal stem cells. Eye 1989;3:141-57.
6. Nishida K. Tissue engineering of the cornea. Cornea 2003;22:Suppl 7:S28-S34.

7. Kenyon KR, Tseng SC. Limbal autograft transplantation for ocular surface disorders. Ophthalmology 1989;96:709-22.
8. Chen JJ, Tseng SC. Corneal epithelial wound healing in partial limbal deficiency. Invest Ophthalmol Vis Sci 1990;31:1301-14.
9. Dua HS, Azuara-Blanco A. Autologous limbal transplantation in patients with unilateral corneal stem cell deficiency. Br J Ophthalmol 2000;84:273-8.
10. Tsubota K, Satake Y, Kaido M, et al. Treatment of severe ocular-surface disorders with corneal epithelial stem-cell transplantation. N Engl J Med 1999;340:1697-703.
11. Samson CM, Nduaguba C, Baltatzis S, Foster CS. Limbal stem cell transplantation in chronic inflammatory eye disease. Ophthalmology 2002;109:862-8.
12. Ilari L, Daya SM. Long-term outcomes of keratolimbal allograft for the treatment of severe ocular surface disorders. Ophthalmology 2002;109:1278-84.
13. Shimazaki J, Shimmura S, Fujishima H, Tsubota K. Association of preoperative tear function with surgical outcome in severe Stevens-Johnson syndrome. Ophthalmology 2000;107:1518-23.
14. Schwab IR, Reyes M, Isseroff RR. Successful transplantation of bioengineered tissue replacements in patients with ocular surface disease. Cornea 2000;19:421-6.
15. Tsai RJ, Li LM, Chen JK. Reconstruction of damaged corneas by transplantation of autologous limbal epithelial cells. N Engl J Med 2000;343:86-93.
16. Rama P, Bonini S, Lambiase A, et al. Autologous fibrin-cultured limbal stem cells permanently restore the corneal surface of patients with total limbal stem cell deficiency. Transplantation 2001;72:1478-85.
17. Nakamura T, Endo K, Cooper LJ, et al. The successful culture and autologous transplantation of rabbit oral mucosal epithelial cells on amniotic membrane. Invest Ophthalmol Vis Sci 2003;44:106-16.
18. Kinoshita S, Nakamura T. Development of cultivated mucosal epithelial sheet transplantation for ocular surface reconstruction. Artif Organs 2004;28:22-7.
19. Yamato M, Okano T. Cell sheet engineering. Mater Today 2004;May:42-7.
20. Kawasaki S, Nishida K, Sotozono C, Quantock AJ, Kinoshita S. Conjunctival inflammation in the chronic phase of Stevens-Johnson syndrome. Br J Ophthalmol 2000;84:1191-3.
21. Foster CS, Fong LP, Azar D, Kenyon KR. Episodic conjunctival inflammation after Stevens-Johnson syndrome. Ophthalmology 1988;95:453-62.
22. Hirose M, Kwon OH, Yamato M, Kikuchi A, Okano T. Creation of designed shape cell sheets that are noninvasively harvested and moved onto another surface. Biomacromolecules 2000;1:377-81.
23. Nishida K, Yamato M, Hayashida Y, et al. Functional bioengineered corneal epithelial sheet grafts from corneal stem cells expanded ex vivo on a temperature-responsive cell culture surface. Transplantation 2004;77:379-85.
24. Jones PH, Watt FM. Separation of human epidermal stem cells from transit amplifying cells on the basis of differences in integrin function and expression. Cell 1993;73:713-24.
25. Pellegrini G, Dellambra E, Golisano O, et al. p63 Identifies keratinocyte stem cells. Proc Natl Acad Sci U S A 2001;98:3156-61.
26. Fantes FE, Hanna K, Waring GO III, Pouliquen Y, Thompson KP, Salvodelli M. Wound healing after excimer laser keratomileusis (photorefractive keratectomy) in monkeys. Arch Ophthalmol 1990;108:665-75.
27. Moll R, Franke WW, Schiller DL, Geiger B, Krepler R. The catalog of human cytokeratins: patterns of expression in normal epithelia, tumors and cultured cells. Cell 1982;31:11-24.
28. Shore JW, Foster CS, Westfall CT, Rubin PA. Results of buccal mucosal grafting for patients with medically controlled ocular cicatricial pemphigoid. Ophthalmology 1992;99:383-95.
29. Dua HS, Joseph A, Shanmuganathan VA, Jones RE. Stem cell differentiation and the effects of deficiency. Eye 2003;17:877-85.
30. Kinoshita S, Friend J, Thoft RA. Sex chromatin of donor corneal epithelium in rabbits. Invest Ophthalmol Vis Sci 1981;21:434-41.
31. Holland EJ, Schwartz GS. Epithelial stem-cell transplantation for severe ocular-surface disease. N Engl J Med 1999;340:1752-3.
32. Shimazaki J, Kaido M, Shinozaki N, et al. Evidence of long-term survival of donor-derived cells after limbal allograft transplantation. Invest Ophthalmol Vis Sci 1999;40:1664-8.
33. Williams KA, Brereton HM, Aggarwal R, et al. Use of DNA polymorphisms and the polymerase chain reaction to examine the survival of a human limbal stem cell allograft. Am J Ophthalmol 1995;120:342-50.
34. Hiscott P, Sorokin L, Nagy ZZ, Schlotzer-Schrehardt U, Naumann GO. Keratocytes produce thrombospondin 1: evidence for cell phenotype-associated synthesis. Exp Cell Res 1996;226:140-6.
35. Rheinwald JG, Green H. Serial cultivation of strains of human epidermal keratinocytes: the formation of keratinizing colonies from single cells. Cell 1975;6:331-43.

POSTING PRESENTATIONS AT MEDICAL MEETINGS ON THE INTERNET

Posting an audio recording of an oral presentation at a medical meeting on the Internet, with selected slides from the presentation, will not be considered prior publication. This will allow students and physicians who are unable to attend the meeting to hear the presentation and view the slides. If there are any questions about this policy, authors should feel free to call the *Journal*'s Editorial Offices.

Available online at www.sciencedirect.com
SCIENCE DIRECT®
Surface Science 570 (2004) 134–141
SURFACE SCIENCE
www.elsevier.com/locate/susc

Incorporation of new carboxylate functionalized co-monomers to temperature-responsive polymer-grafted cell culture surfaces

Mitsuhiro Ebara [a], Masayuki Yamato [b], Shigeru Nagai [b], Takao Aoyagi [b], Akihiko Kikuchi [b], Kiyotaka Sakai [a], Teruo Okano [b,*]

[a] *Department of Applied Chemistry, Waseda University, 3-4-1 Ohkubo, Shinjuku-ku, Tokyo 169-8555, Japan*
[b] *Institute of Advanced Biomedical Engineering and Science, Tokyo Women's Medical University, 8-1 Kawada-cho, Shinjuku-ku, Tokyo 162-8666, Japan*

Available online 10 July 2004

Abstract

Several cultured cell types are easily detached from poly(*N*-isopropylacrylamide) (PIPAAm)-grafted surfaces only by reducing culture temperature without traditional proteolytic treatments that might damage certain cell functions. We have exploited these novel surfaces for tissue engineering applications where harvested intact cell sheets are useful for fabricating tissue-like constructs. We now extend the polymer chemistry of such grafted surfaces with new charged co-monomers. Functional carboxylate groups are incorporated into temperature-responsive surfaces with newly designed analogous carboxylate co-monomers, 2-carboxyisopropylacrylamide (CIPAAm) and 3-carboxy-*n*-propylacrylamide (CNPAAm), which have a small structural difference in the placement of the carboxylate group (*iso* or *normal* to the monomer propyl group). P(IPAAm-*co*-CIPAAm) demonstrates a similar phase transition behavior to that of pure PIPAAm, and the ionic dissociation of carboxyl groups is suppressed (elevated pK'a) even under physiological conditions. By contrast, P(IPAAm-*co*-CNPAAm) exhibits a higher charge density (lower pK'a), higher hydration, and reduced temperature-sensitivity under identical conditions. Introduction of 5 mol% CNPAAm into PIPAAm grafted surfaces produces no cell attachment under typical cell culture conditions, while identical introductions of CIPAAm into grafted copolymers functions well for cell attachment. Cultured cell spreading efficiency was essentially similar on PIPAAm-grafted surfaces as on copolymer-grafted surfaces with 1 mol% introduction of either carboxylate co-monomer. Accelerated cell detachment upon reducing culture temperature was observed for the 1 mol% these copolymer-grafted surfaces since polymer hydration and swelling kinetics are enhanced by the increased ionizable moiety in these grafted surfaces.

* Corresponding author. Tel.: +81 3 3353 8111x30233; fax: +81 3 3359 6046.
E-mail address: tokano@abmes.twmu.ac.jp (T. Okano).

0039-6028/$ - see front matter © 2004 Elsevier B.V. All rights reserved.
doi:10.1016/j.susc.2004.06.183

Keywords: Carboxylic acid; Surface structure, morphology, roughness, and topography

1. Introduction

Poly(*N*-isopropylacrylamide) (PIPAAm) is a water-soluble polymer below its lower critical solution temperature (LCST) of 32 °C [1,2]. This polymer becomes hydrophobic and undergoes reversible phase separation as temperature increases above the LCST. Over the past decade, a considerable number of studies have demonstrated new biomedical applications for PIPAAm, such as intelligent surfaces for bioseparation systems [3,4] and enzyme-free cell culture/harvest systems [5–7]. We have succeeded in surface interaction control with bioactive molecules and cultured cells by exploiting the reversible, temperature-sensitive properties of PIPAAm-grafted surfaces [3–10]. Functionalization of PIPAAm has also been attempted by co-polymerization of IPAAm with other functional co-monomers such as acrylic acid (AAc) [11–13]. However, introduction of other co-monomers often results in reduced temperature sensitivity [14–16]. Particularly, IPAAm copolymers with AAc exhibit a dramatically decreased magnitude of the polymer temperature-sensitive phase transition under physiological conditions (pH 7.4), rendering them impractical for many applications.

In order to overcome these shortcomings, we have designed new functionalized monomers based on the hypothesis that the sharp phase transition behavior observed for PIPAAm results from the alignment of side chain isopropyl groups upon dehydration. We have therefore synthesized 2-carboxyisopropylacrylamide (CIPAAm) having a similar side chain structure of IPAAm [16,17]. IPAAm co-polymers with CIPAAm show sensitive phase transition in response to temperature change, and the LCST is almost the same as that of the IPAAm homopolymer. We have now newly synthesized the analogous monomer, 3-carboxyl-*n*-propylacrylamide (CNPAAm). The only difference from CIPAAm is the propyl side group: *iso*-versus *normal* (see Fig. 1), producing a distinct structural difference in the alignment of the side chain propyl group under hydration, and allowing us to test the hypothesis that this will affect the polymer phase transition. The phase transition behavior and temperature-responsive cell attachment/detachment on these copolymer-grafted surfaces were examined and compared. Distinct differences are observed, allowing us to conclude that the side chain functional group position is important to retain thermally sensitive properties while providing functional co-monomer chemistry.

2. Materials and methods

2.1. Monomer preparation

N-Isopropylacrylamide (IPAAm) was kindly provided from Kojin Co. (Tokyo, Japan) and puri-

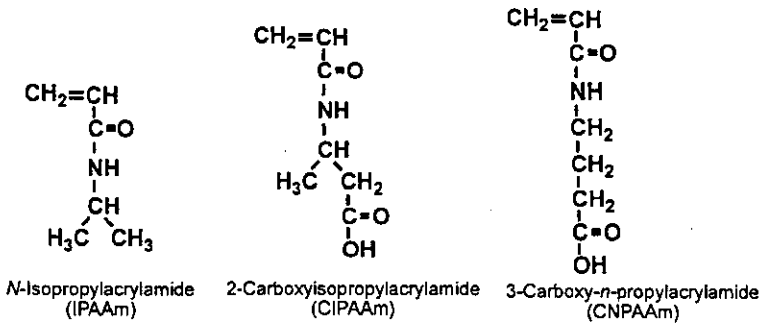

Fig. 1. Chemical structures for *N*-isopropylacrylamide (IPAAm), 2-carboxyisopropylacrylamide (CIPAAm), and 3-carboxy-*n*-propylacrylamide (CNPAAm) monomers.

fied by recrystallization from *n*-hexane. CIPAAm monomer was synthesized as described previously [16]. Briefly, D,L-3-aminobutyric acid (purity 98%, Tokyo Kasei, Tokyo, Japan) was esterified using benzyl alcohol. Acryloyl chloride was reacted with the benzyl ester in the presence of triethylamine. CIPAAm was obtained by hydrolysis of the benzyl ester using sodium hydroxide aqueous solution. Protonation of carboxyl groups was carried out using an excess amount of hydrochloric acid. CNPAAm monomer was similarly synthesized but using D,L-4-aminobutyric acid in place of D,L-3-aminobutyric acid. Both monomers were certified by NMR and were stored as viscous oil at 4 °C under nitrogen prior to polymerization.

2.2. Synthesis of IPAAm copolymers and copolymer-grafted surfaces

IPAAm co-polymers with each functional carboxylate monomer were synthesized as previously reported [16]. Briefly, purified IPAAm, co-monomer, and 2,2′-azobisisobutyronitrile (AIBN) as a free-radical initiator were dissolved in freshly distilled *N*,*N*-dimethylformamide (DMF). The ampoules containing the solution were de-gassed and then sealed by conventional methods, and immersed in a water bath held at 70 °C for 3 h. Copolymers were recovered by repeated precipitation into diethylether followed by drying as white powders. IPAAm copolymer-grafted dishes were prepared as previously reported [5,17]. Briefly, IPAAm monomer was dissolved in 2-propanol at a concentration of 55% (wt/wt). For preparation of IPAAm copolymer-grafted surfaces, either CIPAAm or CNPAAm monomer was added in ratios of 1, 3 and 5 mol% to total monomer concentration in 2-propanol. These monomer solutions were spread uniformly over tissue culture polystyrene dishes (TCPS) dishes (Falcon 3001, Becton Dickinson Labware, Oxnard, CA) and then electron-beam irradiated using an area beam electron processing system (Curetron EBC-200-AA2, Nissin High Voltage Co. Ltd., Kyoto, Japan) at a radiation dose of 0.3 MGy (acceleration voltage of 150 kV under 1.0×10^{-4} Pa). Monomers were polymerized and covalently grafted onto dish surfaces by this electron beam irradiation. Unreacted monomer and ungrafted polymer were then removed by washing extensively with cold water. The amount of grafted polymer was determined by attenuated total reflection Fourier transform infrared spectrophotometry (ATR-FTIR) as previously described [17]. Since the base substrate comprises TCPS, absorption at 1600 cm^{-1} results from the TCPS mono-substituted aromatic ring. As PIPAAm and its copolymers are grafted onto the TCPS surface, strong amide absorption appears in the region of 1650 cm^{-1}. The peak intensity ratio (I_{1650}/I_{1600}) was used to determine grafted density on the surface using the calibration curve of a known PIPAAm amount cast onto TCPS from solution.

2.3. Apparent pK′a measurements for new monomers and respective copolymers

Apparent dissociation constants (K'a) of the carboxylate-containing copolymers were determined from titration using the Henderson-Hasselbalch equation [18]. Each copolymer (100 mg) was dissolved in 10 ml of water, and 2 ml of 0.1 N HCl was added (final pH = 10) so that all carboxyl groups remained in the acid form. Typical carboxylate pK'a for AAc is 4.26. Then, ionized carboxyl groups and added HCl were titrated with 0.05 N NaOH(aq) under nitrogen. The pH where half the carboxyl groups in each copolymer were dissociated stoichiometrically was defined as the apparent pK'a.

2.4. Fluorescence measurements to determine phase transitions

Aqueous phase transition changes for all copolymers across their LCST values were determined by fluorescent measurements [19,20]. Pyrene was used as a hydrophobic fluorescent probe [21]. Fluorescent spectra were recorded on a spectrofluorometer (FP-770, Japan Spectroscopic Co., Tokyo, Japan). The temperature in a water-jacketed cell was controlled with a thermostated circulating bath to ±0.1 °C. Pyrene dissolved in acetone (2.0×10^{-4} M, 10 μl) was added to 4 ml of aqueous polymer solutions (2.5 mg/ml) in Dulbecco's phosphate buffered saline (PBS, pH 7.4). These samples

containing pyrene (5×10^{-7} M) were kept for 24 h at 20 °C before any measurements to allow complete evaporation of acetone. Fluorescence spectra of pyrene solutions contain a vibrational band exhibiting high sensitivity to the polarity of the pyrene environment [22]. From pyrene emission spectra, the intensity (peak height) ratios (I_1/I_3) of the first band (I_1: 374 nm) to the third band (I_3: 385 nm) were plotted as a function of temperature.

2.5. Water contact angle measurements as a function of time and temperature

IPAAm copolymer-grafted TCPS dishes were cut in size to 1.0×3.0 cm. Water contact angle was determined by the sessile drop method with a FACE contact angle meter (image processing type CA-X, Kyowa Interface Science, Saitama, Japan) using Dulbecco's modified Eagle's medium (DMEM, Iwaki, Chiba, Japan). The temperature was controlled by circulating water from a thermostated water bath (±0.1 °C). All samples were measured five times and averaged. Temperature was continuously recorded in situ.

2.6. Cell attachment/detachment assay

Bovine aortic endothelial cells (BAECs) were provided by Health Science Research Resources Bank (JCRB 0099; Osaka, Japan). BAECs were maintained on TCPS dishes with DMEM supplemented with 10% fetal bovine serum (FBS), 100 units/ml penicillin, and 100 μg/ml streptomycin at 37 °C in humidified atmosphere with 5% CO_2. After expansion, BAECs were harvested from TCPS dishes by treatment with 0.25% trypsin-0.26 mM EDTA in PBS. These cells were then plated onto the copolymer-grafted TCPS dishes at a density of 1.0×10^4 cells/cm^2 and cultured at 37 °C. Cell morphology was observed at certain time points and microphotographed under a phase contrast microscope. Spread cell numbers were counted on printed photographs. The ratio of spread cell density on copolymer-grafted surface to that on PIPAAm-grafted surface were presented as relative spread cell density. For low temperature treatments, spread cells were transferred to a CO_2 incubator equipped with a cooling unit fixed at 20 °C. The percentages of detached cell numbers after 30-min incubation at 20 °C to the total cell numbers visible were presented as detached cell ratios. All experiments were performed in triplicate and averaged. Statistics were calculated using SigmaStat 10.0 (SPSS, Chicago, IL).

3. Results and discussion

3.1. Copolymer phase transition behaviors

Temperature-responsive changes of P(IPAAm-*co*-CIPAAm) (CIPAAm 4.8 mol%) and P(IPAAm-*co*-CNPAAm) (CNPAAm 4.0 mol%) were examined using pyrene as a hydrophobic probe [21]. Fig. 2 shows the fluorescence intensity ratios (I_1/I_3) reflecting microenvironmental hydrophobicity surrounding pyrene [22]. Low I_1/I_3 values resulted from polymer collapsed hydrophobic environments, that is, polymer chains are hydrophobic and aggregate to change probe partitioning and fluorescence. PIPAAm solutions showed

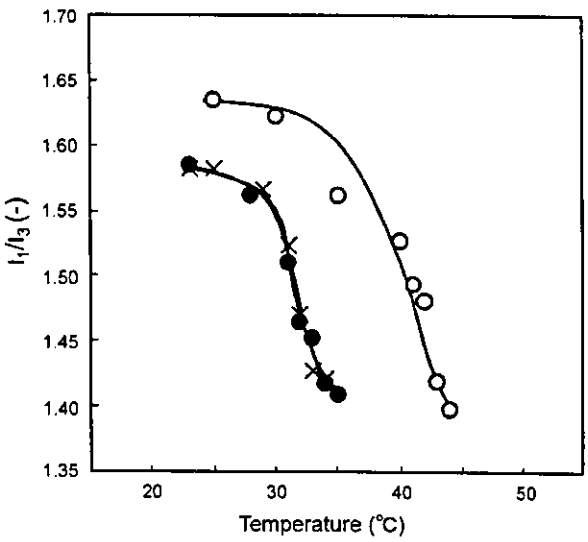

Fig. 2. Fluorescence measurements of IPAAm-based copolymer solutions at pH 7.4. The fluorescence intensity ratio I_1/I_3 reflects the microenvironmental hydrophobicity surrounding pyrene [22]. Pure PIPAAm: crosses, P(IPAAm-*co*-CIPAAm) (CIPAAm content 4.8 mol%): closed circles, P(IPAAm-*co*-CNPAAm) (CNPAAm content 4.0 mol%): open circles.

abrupt decreases in their I_1/I_3 values when temperature increased across its LCST of 32 °C, indicating the hydrophobic changes of polymer chains [19,20]. P(IPAAm-*co*-CIPAAm) solutions also showed similar abrupt decreases in this ratio when temperature was increased across 32 °C. Introduction of 4.8 mol% CIPAAm to PIPAAm did not alter the original LCST (see Fig. 2). This is asserted to result from strong monomer structural similarities and the resulting uninterrupted sequences of isopropyl side groups in both homo- and co-polymers. In contrast, P(IPAAm-*co*-CNPAAm) copolymers showed higher polarity ratios than PIPAAm solutions at any temperature, suggesting a weaker hydrophobic interaction among copolymer side chains, weaker aggregated collapse and elevated LCST above 32 °C. This could be produced by the different carboxylate side chain group position that cannot permit isopropyl side chain alignment and cooperative collapse with IPAAm-based copolymer after LCST dehydration as in the CIPAAm case.

The pK'a value for the P(IPAAm-*co*-CIPAAm) copolymer was considerably higher than that for P(IPAAm-*co*-CNPAAm), while the CIPAAm monomer's pK'a was very similar to that of CNPAAm (Table 1). Specifically, carboxyl groups in the copolymer exhibit suppressed dissociation at pH 7.4 at 10 °C below the LCST. This could result from cooperative hydrophobic interactions among isopropyl groups that either lower the local dielectric environment of the side chains, promote known carboxylate hydrogen bonded dimerization in this environment, or restrain repulsive forces between dissociated carboxyl groups. Fig. 3 shows pK'a values observed for IPAAm copolymers plotted against solution temperature. At any temperature, P(IPAAm-*co*-CNPAAm) exhibits higher acidity than P(IPAAm-*co*-CIPAAm). Each copolymer has constant acidity below its LCSTs. But, solution acidity increases with temperature to 47 °C for the P(IPAAm-*co*-CNPAAm) copolymer. These observations are consistent with the copolymer hydrophobicity increasing with increasing temperature above their respective LCSTs [14, 23,24]. These would result from protonation of carboxyl groups and subsequent hydrophobic aggregation for P(IPAAm-*co*-CNPAAm), distinct from the other polymers tested. The solution pK'a increase for P(IPAAm-*co*-CIPAAm) over this temperature increase was small, reflecting reduced dissociation of carboxyl groups in P(IPAAm-*co*-CIPAAm) solutions. These results clearly indicate the physicochemical affects of the slight structural difference between these two monomers (*iso*-propyl versus *normal*-propyl), and the resulting significant differences in their phase transition behaviors when introduced into copolymers. The pK'a for IPAAm-AAc copolymers is around 5 [14,23,24],

Table 1
Apparent pK'a values measured by titration at 10 °C

Samples	pK'a
CIPAAm monomer	4.58
CNPAAm monomer	4.70
P(IPAAm-*co*-CIPAAm) (CIPAAm 4.8 mol%)	6.17
P(IPAAm-*co*-CNPAAm) (CNPAAm 4.0 mol%)	4.90

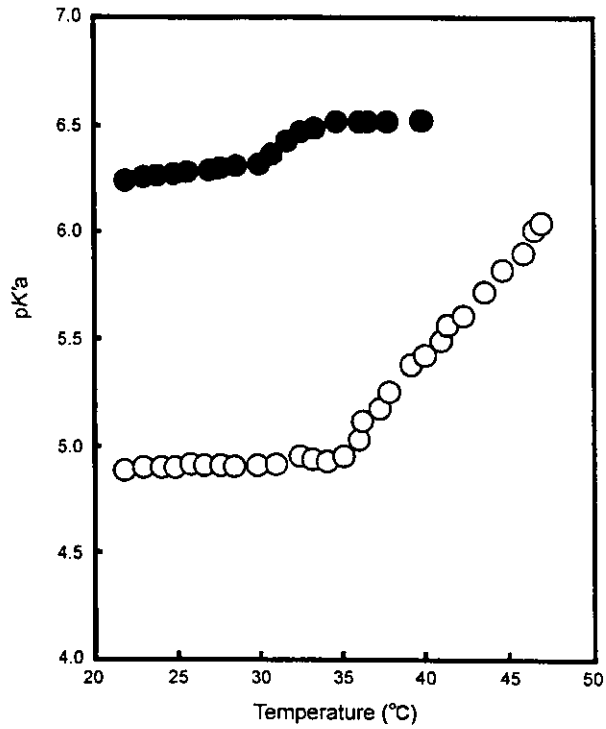

Fig. 3. Temperature dependence for apparent pK'a values for IPAAm-based copolymers. P(IPAAm-*co*-CIPAAm) (CIPAAm content 4.8 mol%): closed circles, P(IPAAm-*co*-CNPAAm) (CNPAAm content 4.0 mol%): open circles.

which is close to the pK'a for P(IPAAm-*co*-CNPAAm).

3.2. Cell spreading and detachment on polymer-grafted surfaces in culture

PIPAAm, P(IPAAm-*co*-CIPAAm), and P(IPAAm-*co*-CNPAAm) were polymerized in situ and covalently grafted onto TCPS surfaces by electron beam irradiation. The graft amounts estimated by ATR-FTIR were approximately 1.8–1.9 μg/cm^2. We have reported attachment, spreading and detachment results for BAECs on pure PIPAAm-grafted surfaces. These results indicate that BAECs attach and spread normally on the PIPAAm homopolymer-grafted culture surface above the polymer LCST, and detach readily once below the LCST [5]. Fig. 4 shows BAEC spreading after 2-day culture at 37 °C on these surfaces. On copolymer-grafted surfaces, cell spreading was continually and increasingly hindered with increasing CNPAAm content in copolymer grafts. No BAEC attachment or spreading was ever obtained on copolymer-grafted surfaces containing 5 mol% feed-ratio of CNPAAm. Interestingly, BAEC spreading was not influenced by the introduction of analogous CIPAAm up to 5 mol% feed ratio. These observations are consistent with the observed phase transition data for these copolymers. P(IPAAm-*co*-CNPAAm) exhibits significant hydrophilicity even at 37 °C similar to P(IPAAm-*co*-CIPAAm) below its LCST shown already to repel cell attachment even in serum-supplemented culture media (see Fig. 2 and Ref. [17]).

Cell detachment upon reducing culture temperatures to 20 °C was examined with both PIPAAm- and copolymer-grafted surfaces with co-monomer composition controlled to 1 mol% feed ratios. Spread cell densities at 37 °C were nearly identical (see Fig. 4). Fig. 5 shows the time course of wettability changes of each grafted surface in response to decreasing temperature changes from 37 to 20 °C. All polymer-grafted surfaces showed similar wettability at 37 °C and became more hydrophilic (more wettable) in response to the temperature reduction. This is due to the common polymer chain hydration that occurs below the LCST. Both P(IPAAm-*co*-CIPAAm) and P(IPAAm-*co*-CNPAAm)-grafted surfaces demonstrated more rapid and larger hydrophobic to hydrophilic

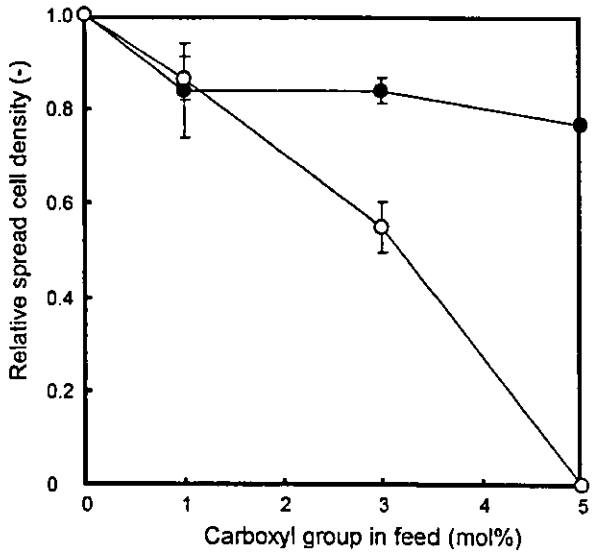

Fig. 4. Relative spread cell densities in culture. BAECs were seeded on IPAAm-based copolymer-grafted TCPS dishes and cultured for 2 days at 37 °C in serum-containing media (see text for details). P(IPAAm-*co*-CIPAAm) grafted surfaces: closed circles, P(IPAAm-*co*-CNPAAm) grafted surfaces: open circles.

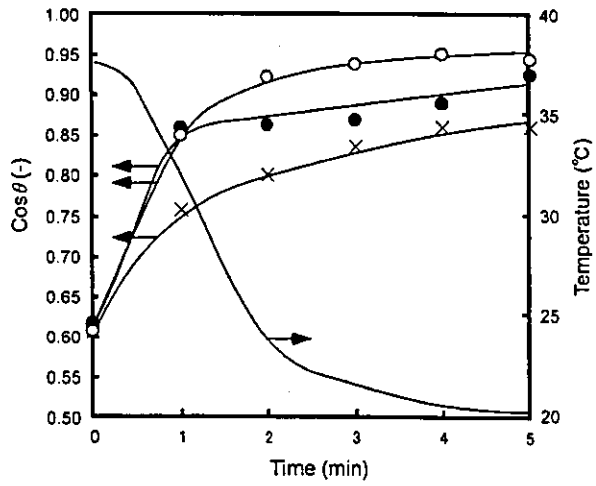

Fig. 5. Surface wettability changes for IPAAm-based grafted surfaces versus time and temperature. Advancing contact angles θ of all samples were measured 5 times with the sessile aqueous droplet technique and plotted as mean values ± S.D. Pure PIPAAm: crosses, P(IPAAm-*co*-CIPAAm) grafted surfaces (CIPAAm 1 mol% in feed): closed circles, P(IPAAm-*co*-CNPAAm) grafted surfaces (CNPAAm 1 mol% in feed): open circles.

changes in their surface properties than PIPAAm-grafted surfaces, indicating carboxyl groups in the copolymer cause a rapid and excessive hydration of both types of polymer chains below their LCSTs. P(IPAAm-*co*-CNPAAm)-grafted surfaces were more hydrophilic (lower contact angle with water) than P(IPAAm-*co*-CIPAAm)-grafted surfaces at 20 °C. This could reflect the observed p*K'*a for P(IPAAm-*co*-CNPAAm) at 20 °C being lower than that for P(IPAAm-*co*-CIPAAm) (see Fig. 3) and is also consistent with the assertion that ionized carboxyl groups likely produce rapid and excess hydration of the grafted surface since the PIPAAm homopolymer grafted surface does not behave this way. Fig. 6 shows the detached cell to total cell ratios after lowering culture temperatures to 20 °C. Rapid cell detachment is observed on the surfaces grafted with P(IPAAm-*co*-CIPAAm) and P(IPAAm-*co*-CNPAAm). This result corresponds to the observed hydrophilicity on these surfaces at 20 °C and the rapid swelling kinetics for these charged polymer surfaces predicted from these data below the LCST.

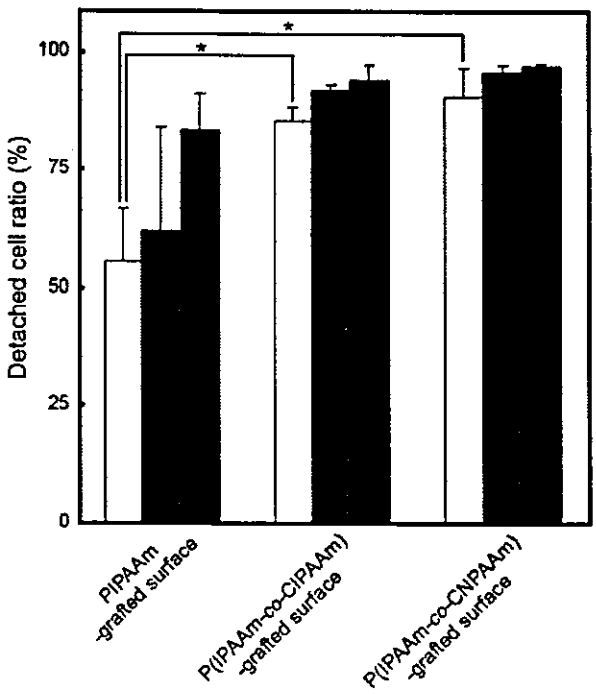

Fig. 6. Cell detachment upon reducing culture temperature to 20 °C. Percentage of detached cells to total cells prior to lowering temperature is plotted for grafted TCPS surfaces containing pure PIPAAm, P(IPAAm-*co*-CIPAAm) (1 mol% CIPAAm in feed), and P(IPAAm-*co*-CNPAAm) (1 mol% CNPAAm in feed). Remaining cell numbers counted after 30- (white), 60- (gray), and 90-min (black) incubations at 20 °C are shown. Statistically significant differences are indicated using Bonferroni test (*, $P<0.01$).

4. Conclusions

A newly synthesized and novel carboxylate-containing acrylamide monomer, CNPAAm, was characterized in thermally sensitive co-polymer grafted surfaces. Temperature-responsive behavior for both P(IPAAm-*co*-CNPAAm) and P(IPAAm-*co*-CIPAAm) were compared. The detected p*K'*a for P(IPAAm-*co*-CIPAAm) was considerably higher than that for P(IPAAm-*co*-CNPAAm) and other previously reported carboxylate co-polymers [14,23,24]. This reflects reduced or hindered carboxylate group dissociation in the P(IPAAm-*co*-CIPAAm) copolymer. Furthermore, temperature-dependent association/dissociation changes in copolymer carboxylate groups in P(IPAAm-*co*-CIPAAm) were smaller than those observed in P(IPAAm-*co*-CNPAAm). Slight structural differences between the two analogous monomers (*iso* or *normal* side group substitutions) are asserted to produce these significant differences in thermally induced phase transition behaviors of their IPAAm copolymers and are correlated with observed apparent p*K'*a values and contact angle results. Spread cell density on P(IPAAm-*co*-CNPAAm)-grafted surface above its LCST decreased with increasing CNPAAm content because of its LCST shift to higher temperature above 37 °C correlated with its lower apparent p*K'*a, higher hydrophilicity and resulting higher content of ionized carboxyl groups below the LCST. Because the LCST value for P(IPAAm-*co*-CIPAAm) is not altered significantly by CIPAAm content [23], spread cell density above 37 °C is not significantly affected by increasing temperature and is comparable to the PIPAAm-grafted surface for cell attachment and detachment performance. By contrast, incorporation of the carboxylate co-monomers into PIPAAm-grafted surfaces similarly accelerates cultured cell detachment below the respective polymer LCST.

Acknowledgments

We appreciate the continued useful comments and technical criticism from Prof. D.W. Grainger (Colorado State University, USA). This work is supported in part by Grants-in-Aid for Scientific Research by Ministry of Education, Culture, Sports, Science and Technology of Japan. The present study is supported in part by Japan Ministry for Culture, Sports, Education, Science and Technology, Core Research for Evolutional Science and Technology (CREST).

References

[1] Y.H. Bae, T. Okano, S.W. Kim, J. Polym. Sci. Part B: Polym. Phys. 28 (1990) 923.
[2] M. Heskins, J.E. Guillet, J. Macromol. Sci. Chem. A2 (1968) 1441.
[3] H. Kanazawa, K. Yamamoto, Y. Matsushima, N. Takai, A. Kikuchi, Y. Sakurai, T. Okano, Anal. Chem. 68 (1996) 100.
[4] H. Feil, Y.H. Bae, J. Feijen, S.W. Kim, J. Membrane Sci. 64 (1991) 283.
[5] T. Okano, N. Yamada, H. Sakai, Y. Sakurai, J. Biomed. Mater. Res. 27 (1993) 1243.
[6] T. Shimizu, M. Yamato, Y. Isoi, T. Akutsu, T. Setomaru, K. Abe, A. Kikuchi, M. Umezu, T. Okano, Circ. Res. 90 (2002) e40.
[7] M. Yamato, M. Utsumi, A. Kushida, C. Konno, A. Kikuchi, T. Okano, Tissue Engng. 7 (2001) 473.
[8] M. Yamato, C. Konno, A. Kushida, M. Hirose, M. Utsumi, A. Kikuchi, T. Okano, Biomaterials 21 (2000) 981.
[9] K. Yoshizako, K. Akiyama, H. Yamanaka, Y. Shinohara, Y. Hasegawa, A. Kikuchi, T. Okano, Anal. Chem. 74 (2002) 4160.
[10] T. Yakushiji, K. Sakai, A. Kikuchi, T. Aoyagi, Y. Sakurai, T. Okano, Anal. Chem. 71 (1999) 1125.
[11] G. Chen, A.S. Hoffman, Nature 373 (1995) 49.
[12] G. Chen, A.S. Hoffman, Macromol. Chem. Phys. 196 (1995) 1251.
[13] H. Yu, D.W. Grainger, J. Appl. Polym. Sci. 49 (1993) 1553.
[14] H. Feil, Y.H. Bae, J. Feijan, S.W. Kim, Macromolecules 26 (1993) 2496.
[15] Y. Kaneko, S. Nakamura, K. Sakai, T. Aoyagi, A. Kikuchi, Y. Sakurai, T. Okano, Macromolecules 31 (1998) 6099.
[16] T. Aoyagi, M. Ebara, K. Sakai, Y. Sakurai, T. Okano, J. Biomater. Sci. Polymer Edn. 11 (2000) 101.
[17] M. Ebara, M. Yamato, M. Hirose, T. Aoyagi, A. Kikuchi, K. Sakai, T. Okano, Biomacromolecules 4 (2003) 344.
[18] A. Katchalsky, P. Spitnik, J. Polym. Sci. 2 (1947) 432.
[19] J.E. Chung, M. Yokoyama, K. Suzuki, T. Aoyagi, Y. Sakurai, T. Okano, J. Colloid. Surf. B: Biointerfaces 9 (1997) 37.
[20] F. Kohori, K. Sakai, T. Aoyagi, M. Yokoyama, Y. Sakurai, T. Okano, J. Control. Rel. 55 (1998) 87.
[21] K. Kalyanasundaram, J.K. Thomas, J. Am. Chem. Soc. 99 (1977) 2039.
[22] D.C. Dong, M.A. Winnik, Can. J. Chem. 62 (1984) 2560.
[23] H. Feil, Y.H. Bae, J. Feijan, S.W. Kim, Macromolecules 25 (1992) 5528.
[24] J. Kobayashi, A. Kikuchi, K. Sakai, T. Okano, J. Chromatogr. A 958 (2002) 109.

細胞シート工学を利用した組織再構築

■清水 達也・岡野 光夫
東京女子医科大学 先端生命医科学研究所

Key words：再生医療，組織工学，細胞シート

はじめに

近年，欠損部あるいは機能不全に陥った組織・臓器に対する新たな治療法として再生医療が注目を集め，下肢虚血に対する骨髄単核球細胞移植など細胞を使ったいくつかの治療法が臨床応用されるに至っている。再生医療には細胞を注射針などで不全部に注入する細胞移植療法と組織工学 (tissue engineering) 的手法により細胞から組織を再構築したうえで移植する方法がある。後者はこれまでの医学だけでは実現が困難であった研究領域であり工学的な技術との融合により急速に進歩しつつある。ここでは，組織工学を基盤とした再生医療の現状について概説し，当研究所が開発した独自の組織工学的手法『細胞シート工学』による種々の組織再構築に関する研究を紹介する。

1．組織工学 (tissue engineering)

組織工学は1993年，工学者であるLangerおよび外科医であるVacantiが提唱した学際的な学問である。細胞から組織を再構築するという研究は皮膚などに関してそれ以前より行われていたが，彼らはマウスの背中で耳を再生させたことにより組織工学を世界に知らしめた。組織の再生には細胞，細胞の足場となる細胞外マトリックス (ECM)，細胞の分化・増殖のためのサイトカインが必要であるとし，その足場として3次元の生体吸収性材料を用いた。細胞を3次元の支持体に播種・培養後，生体内に移植すると，生体吸収性の支持体が徐々に分解，細胞が産生するECMと置換され生体に類似した組織が再構築されるという手法である。組織工学において組織再生の足場として用いられる生体材料の多くは生体吸収性の高分子である。これには天然高分子と合成高分子がある。いずれも酵素分解あるいは加水分解によって高分子主鎖が切断され吸収される。天然高分子の中でよく利用されているのは生体のECMの主成分であるコラーゲンである。一方，合成高分子としては，ポリ乳

Cell sheet engineering for tissue reconstruction：Tatsuya Shimizu, Teruo Okano, Institute of Advanced Biomedical Engineering and science, Tokyo Women's Medical University

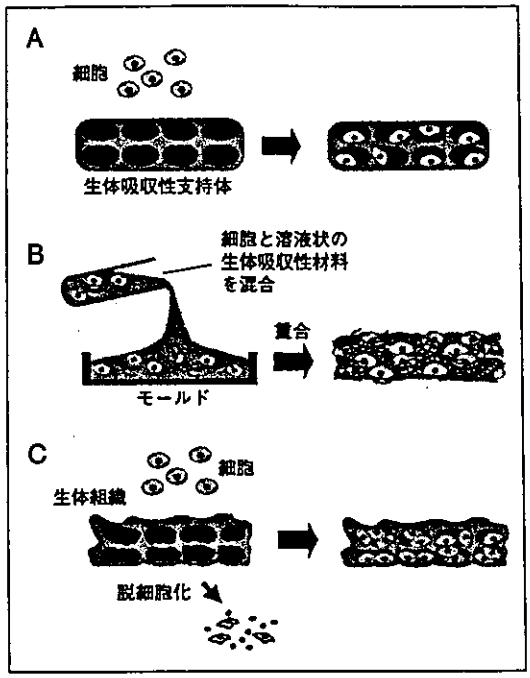

図1　生体吸収性支持体を用いた組織工学的手法
A. 生体吸収性高分子からなる支持体を作成し，それを足場として細胞を播種する手法。
B. 溶液状の支持材料と細胞を混合したのち重合する手法。
C. 生体由来の組織を脱細胞化したのちにそれを支持体として細胞を播種する方法。

酸 (PLA)，ポリグリコール酸 (PGA)，およびそれらの共重合体が最も盛んに使用されている。また，生体由来の組織が支持体として用いられる場合もある。具体的な方法としては①生体吸収性高分子からなる多孔性の3次元支持体を作製，それを足場として細胞を播種する方法（図1 A），②溶液状の生体吸収性材料と細胞を混合したのちモールドに流し込み，重合させることで細胞を3次元化する方法（図1 B），③生体組織を界面活性剤やマイクロウェーブを用いて脱細胞化した結合組織を支持体として細胞を播種し培養する方法（図1 C）がある。それぞれ支持体は生体が産生するECMと置換されて組織が再生される。

これら生体吸収性の3次元生体材料を細胞の足場として用いた組織工学の研究は殆どすべての組織に対して行われている。既に組織工学的に製造された軟骨・皮膚は商品化されており，また血管に関しても臨床応用されている。

2．細胞シート工学による組織再構築

生体吸収性の支持体を用いる組織工学的手法においては支持体内へ十分な細胞を播種することが困難なことやまた移植後支持体の分解に伴い炎症反応が生じることが問題となっている。また骨，軟骨，血管，弁など細胞が疎な組織の作製には適しているが心筋，肝臓など細胞の密な組織を作製するには新たな技術開発が必要となっている。そこで我々は最初から3次元的な足場を整えることにより組織を再生するという既存のコンセプトに対し，温度変化のみで細胞の接着・脱着を制御できる培養基材を用い，細胞をシート状に回収，この細胞シートを一つの組織として移植したり，積層化により3次元組織を再構築したうえで移植するという独自のコンセプト「細胞シート工学」を提唱し新たな治療法の確立に取り組んでいる。

この培養基材は通常のポリスチレン培養皿上に温度応答性高分子であるポリ（*N*-イソプロピルアクリルアミド）を電子線を用いて薄く（数十μm）共有結合させたもので，通常の培養温度である37℃では疎水性表面となり細胞接着性であるが，32℃以下では親水性表面に変化し細胞非接着性となる。この培養皿の使用により，接着した細胞をトリプシンやディスパーゼなどの蛋白分解酵素を用いること

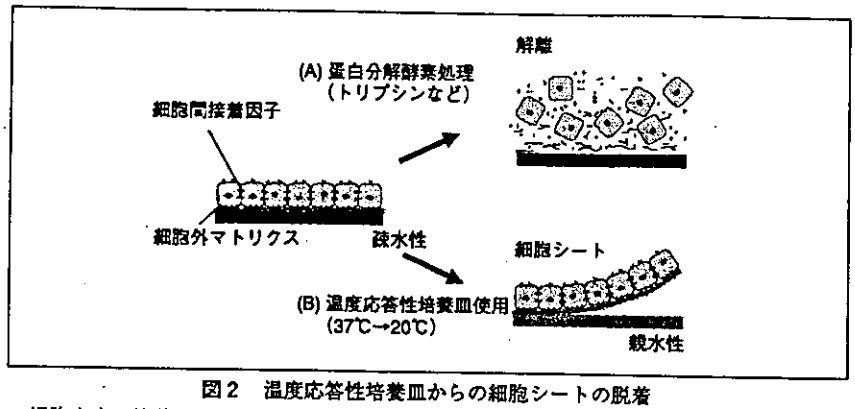

図2　温度応答性培養皿からの細胞シートの脱着

細胞を密に培養した場合は細胞と細胞が細胞間接着因子により互いに接着する。(A) 蛋白分解酵素を用いた場合は細胞と培養皿の接着が解離するとともに，細胞間接着も破壊されるため，それぞれの細胞は解離して浮遊することになる。(B) これに対し，温度応答性培養皿を使った低温処理においてはこの細胞間接着は全く影響を受けずに，シート下面のECMと培養皿表面の接着のみ解離するため細胞がシート状に脱着する。

なく脱着させることが可能である。さらに，細胞を密に培養し細胞が互いに接着した状態では，温度を降下させることにより細胞がその下面の接着因子・ECMとともに培養皿から脱着するものの，細胞間の結合は全く解離せず維持されるため蛋白分解酵素を用いたときのように細胞をばらばらにすることなく，シート状に回収できる（図2）。また細胞シート下面の接着因子が新たな培養基材や別の細胞シート上への移動時に糊の役目を果たすため速やかな接着・積層化が可能である。既にこの培養皿を用い，種々の細胞シートの回収が可能となっている。

細胞シートの再生医療への応用としては①単層シートの移植 ②同一細胞シートの積層化により構築した均一な組織の移植 ③数種の細胞シートの積層化により構築した層状構造を呈する組織の移植がある（図3）。それぞれ対象組織・臓器として ①角膜，膀胱（上皮），歯周組織，②心筋，③肝臓などが挙げられる。以下に，それぞれについてのこれまでの研究成果を示す。

3．単層シート

(1) 角　膜

角膜移植に関しては，ドナー角膜の不足が問題となっており，組織工学的手法による角膜再生が追求されてきた。角膜は組織構造が比較的単純な層構造を呈し，細胞シートによる再生医療のもっとも良い応用例の一つである。我々は，自己の健常側角膜輪部より採取した角膜上皮の幹細胞を温度応答性培養表面上で培養して細胞シートを作製，これを損傷した病変角膜部に移植する治療法を開発した。さらに，両眼性疾患に対しては，自己の口腔粘膜から採取した細胞を用いて細胞シートを作製し移植する方法も確立した。既に本法のヒトへの臨床応用を開始，視力の回復を確認している（大阪大学眼科との共同研究）。

(2) 膀　胱

現在，膀胱機能不全や悪性腫瘍などによる膀胱の欠損に対しては自己の消化管を使用した再建が行われているが，消化管粘膜の残存

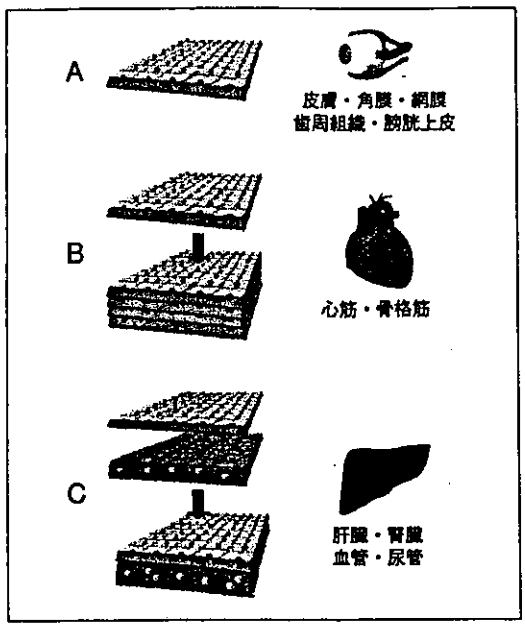

図3　細胞シートの再生医療への応用
温度応答性培養皿から回収した細胞シートの再生医療への応用として3つのコンセプトがある。単層シートの移植(A)。同一の細胞シートを重層化した均一な組織の移植(B)。異なる細胞シートの重層化による層状組織の移植(C)。

に起因する電解質異常，結石の形成などの合併症が大きな問題となっている。これらの問題を解決するために尿路上皮細胞シートを作製し，消化管粘膜を切除した消化管平滑筋層上に移植した。尿路上皮シートは消化管平滑筋層上に生着し，膀胱組織と同様の尿路上皮組織層が再生された。この粘膜置換型フラップは従来の手術方法に細胞シート技術を融合した新規の手法であり，早期の臨床応用が期待されている。

(3) 歯周組織

歯周病は，成人の8割以上が患っているといわれており，歯根膜を中心とする歯周組織の炎症により，放置すれば歯の脱落を招く。従来の治療法では失われた歯周組織は再生することなく，高齢化社会におけるQOL (Quality of Life) の低下の大きな要因といえる。そこで，我々は歯根膜組織由来細胞シートを歯周組織欠損部位へ移植することで，きわめて効果的に歯根組織膜が再生することを明らかとした(東京医科歯科大学歯学部との共同研究)。この技術は歯周組織の再生治療や歯根膜を持った次世代の人工歯根の開発に大きく貢献するものと考えている。

4．同一細胞シートの積層化

心　筋

心筋組織に対する再生医療としては，心筋細胞の代替として自己の筋芽細胞や骨髄由来の細胞を用いた浮遊液注入による細胞移植治療が既に臨床応用されている。一方，組織工学的なアプローチとしてコラーゲンゲル，ポリ乳酸，アルギン酸あるいはゼラチンからなる3次元の支持体を用いた心筋細胞の3次元培養の研究が報告されている。しかし，3次元支持体を用い心筋細胞培養を行うことは細胞の密な接着や自由な収縮弛緩の妨げになると考えられる。そこで我々は心筋細胞シートを重層化することで支持体を用いない心筋組織の再生を追求してきた。重層化した心筋細胞シート間には電気的にも形態的にも結合が生じ，組織全体が同期して拍動することが確認され，*in vitro*で4枚まで積層化したところ肉眼レベルで拍動する心筋組織が構築された。さらにヌードラット背部皮下組織への移植実験を行ったところホストの心電図とは異なるグラフト由来の電位が確認された。また心筋グラフトの肉眼レベルでの拍動が確認さ

れるとともに組織切片上，多数の新生血管を認め，心筋様組織が再生されていた。既に移植後1年まで，心筋グラフトが拍動を維持したまま生着しうることを確認している。さらに重層化心筋細胞シートの心筋梗塞モデルへの移植実験により心機能が改善することが確認されている（大阪大学臓器機能制御外科との共同研究）。将来，幹細胞生物学の発展によりヒトに移植可能な心筋細胞の分化誘導法が確立されれば体外で再生した心筋組織を不全心に移植することも可能となることが予測される。

5．異なる細胞シートの積層化

肝　臓

肝臓は生体内である程度の再生能をもつものの，その形態・機能の複雑さ故に組織工学的手法での再生が困難な組織のひとつである。肝組織は肝実質細胞と血管内皮細胞が層状に配列し，生体内における合成，代謝を効率的に行っている。肝実質細胞は，通常の培養環境ではその分化機能を著しく低下させ，長期培養も困難であることが知られている。そこで肝細胞シートと内皮細胞シートの重層化共培養を行ったところ，アルブミン合成能を維持した2ヶ月以上にわたる肝細胞の長期培養が可能となっている。これは，肝細胞と内皮細胞との層状の接着により生体に似た環境を再現し，細胞相互間のコミニュケーションを可能にしたことによるものと考えられる。この手法を基盤として，3次元的な肝組織を再生・移植するための技術開発を行っている。

以上に挙げた組織・臓器の他，皮膚・網膜・尿管・血管・腎臓などに関しても細胞シートの技術を使った研究を進めている。

おわりに

再生医療は今まで治療が困難であった疾患に対する新たな治療法として期待され，種々のアプローチで開発が行われ，研究者人口も増大している。その中で温度応答性培養皿およびそれを使った細胞シート工学は既存の培養技術では不可能であったシート状の細胞の回収・移動・重層化を実現し世界的にも注目されており，再生医療分野をさらに発展させる新技術として貢献するものと考える。

＜BIO Information＞

第18回 日本臨床内科医学会 in 岡山のお知らせ

会　期：2004年9月19日（日）～20日（月・祝）
会　場：岡山衛生会館・おかやま三光荘・岡山プラザホテル
テーマ：21世紀の理想の医療を目指して
～良質な医療提供とかかりつけ医の役割～
会　長：亀山一郎（亀山内科院長）

主なプログラム：基調講演　医療保険制度と診療報酬体系（講師　遠藤久夫・学習院大学経済学部教授）
インフルエンザの展望（講師　柏木征三郎・福岡日赤血液センター所長）
良質な医療提供とかかりつけ医の役割（講師　伴信太郎・名古屋大学医学部教授）

教育講演／ワークショップ／シンポジウム／市民公開講座　他

Regeneration of Tissues and Organs

— New Technique Opens Up New Possibilities for Regenerative Medicine through Control of Interaction of Polymers with Water —

Institute of Advanced Biomedical Engineering and Science, COE Program for 21st Century, Tokyo Women's Medical University
Associate Professor
KIKUCHI Akihiko

Institute of Advanced Biomedical Engineering and Science, COE Program for 21st Century, Tokyo Women's Medical University
Professor
OKANO Teruo

1 Introduction

Human bodies consist of approximately 60 trillion cells. Such a huge number of cells plays an important role in the formation of the body's tissues and organs. These tissues and organs have a close relationship with each other and express cooperatively various essential functions within the body. When this equilibrium is disturbed, the body becomes sick and treatment is necessary. Although it depends on the particular disease concerned, in some cases treatment can be accomplished by taking medicine alone. In other cases, however, disease can lead to organ dysfunction, which can afflict a person throughout their entire life. In such cases, artificial organs are used to replace damaged ones.

Up until now, much research has been carried out both within Japan and overseas and although artificial organs have been developed that are now in practical use, at present they can only replace some of the functions of the body's organs. Since the 1990s, the concept of tissue engineering has been presented as a development technique for artificial organs as it is more similar to biological organs.[1] Now, tissue engineering research is being actively carried out in numerous places throughout the world with regard to various tissues and organs.[2] In some of the early work in tissue engineering, materials such as poly(lactic acid) (PLA) and poly(lactic-*co*-glycolic acid) (PLGA), which are biodegradable materials, with porous structure, were used to grown target cells. While the cells on these materials divide and proliferate to form tissue, the material itself gradually biodegrades within the living organism to eventually leave only the regenerated tissue. This method is being used to regenerate tissue in the ears and nose, bone and cartilage in the digits, and for the regeneration of other tissue.

In our laboratory we have not been using the technique of transplanting grown cells on biodegradable materials into living organisms, but rather have been taking the cells and tissues that have been grown in newly developed culture dishes and transplanting them directly in single or multiple layers for use in regenerative medicine-related research and clinical applications. In this article we will offer an explanation of the nature and applications of the thermoresponsive surface that we have developed.

2 Surfaces that Change Properties in Response to Changes in Temperature

Since the 1980s, we have been interested in poly(*N*-isopropylacrylamide), hereafter referred to as, "PIPAAm" (Fig. 1) and have been investigating its application as matrices for the drug delivery systems (DDS)[3),4)] and the development of new polymer-enzyme bioconjugates to control enzymatic reactions with thermal stimuli.[5),6)] Surfaces modified with PIPAAm exhibit temperature responsive changes in water: that is hydrophilic behavior at low temperatures and become hydrophobic above 32°C in water,

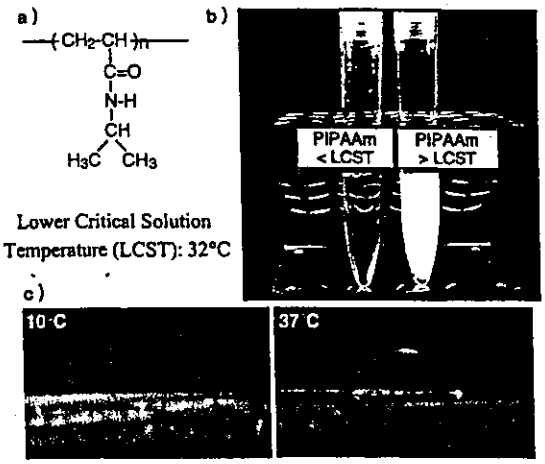

Fig. 1 Characteristics of thermoresponsive poly (*N*-isopropylacrylamide) (PIPAAm)
The chemical structure (a), changes in water solubility in response to temperature changes (b) of PIPAAm, and thermoresponsive wettability changes of PIPAAm-grafted surfaces

showing that it has thermoresponsive characteristics (Fig. 1c).[7),8)]

In order to prepare PIPAAm-modified surfaces you can either use amide bonding between PIPAAm containing carboxyl groups at one chain end and amino groups generated on the surfaces or expose to an electron beam immediately after casting them with IPAAm monomer solution. During the electron beam irradiation, polymerization of the IPAAm monomer and fixation to the surfaces occur simultaneously.[9)] With either method, an ultra-thin layer of PIPAAm grafts is formed on the surface of the material. We ablated the PIPAAm modified surfaces with a low-energy UV excimer laser, peeled back the PIPAAm layer until the original surface of the material was exposed by the absorption of a hydrophobic fluorescent dye. These surfaces were then analyzed with time-of-flight secondary ion mass spectrometry (ToF-SIMS) so that we verified the exposure of the surface of the material. By scanning the ablated area using an atomic force microscope (AFM) we confirmed that the thickness of the surface grafted layer was approximately 20nm (article in press). The amount of the surface grafted polymers was determined using attenuated total reflectance Fourier transform infrared spectroscopy (ATR/FTIR) and found to be approximately 2μg/cm^2, which is very similar to the film thickness as calculated when the specific gravity of PIPAAm is 1. In either case, this would be like stretching a thin membrane with the thickness of a single human hair over the entire width of a baseball stadium and having an ultra thin layer formed on the surfaces of the polymeric base materials.

The PIPAAm modified surfaces respond to changes in environmental temperature due to the thermoresponsive property changes in the PIPAAm grafted molecules, exhibiting hydrophilic behavior at low temperatures while at 32°C the water contact angle changes discontinuously and at high temperatures dehydration of the PIPAAm chains occurs and the surface exhibits hydrophobic behavior (see Fig.1c).

3 Separating Molecules

We have been carrying out joint research together with Prof. Hideko KANAZAWA and her colleagues of Kyoritsu College of Pharmacy, covalent grafting thermoresponsive polymer layers on silica beads in the same way as described above and then placing them in a stainless steel column to create a new chromatography system using only a water as mobile phase.[10~12)] Using this column we were able to control surface hydrophilic/hydrophobic characteristics with temperature, and separate hydrophobic compounds in a mixture of various steroid hormones through the modulation of hydrophobic interaction between column matrix surfaces and steroid hormones with different hydrophobicities (Fig.2). More hydrophobic steroids showed longer retention times, thus a mixture of steroids were successfully separated. Furthermore, we discovered that it is possible to dynamically control column temperature during elution to achieve gradient elution. In other words, after separating solutes with small degree of

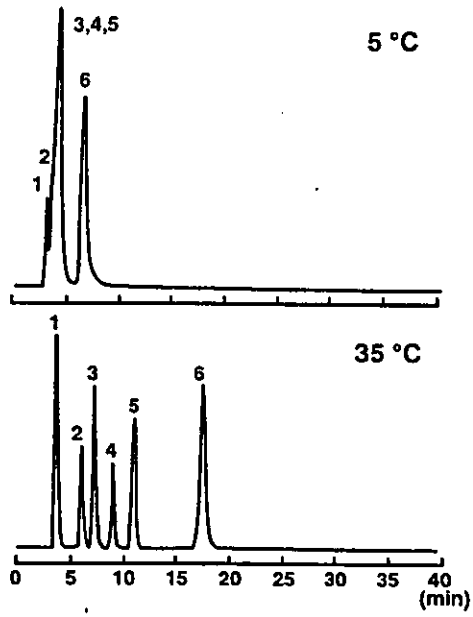

Fig. 2 Changes in the retention behavior of steroids and benzene at various temperatures on a thermoresponsive column. (Eluent: water)

Peaks: 1. Benzene; 2. Hydrocortisone; 3. Prednisolone; 4. Dexamethasone; 5. Hydrocortisone Acetate; 6. Testosterone.

hydrophobicities at high temperature, we lowered the temperature of the column and accelerated the elution by weakening the interaction between the solutes with the high degree of hydrophobicity and the column matrices to achieve a high efficiency separation within a short period of time and realize separation based on the stepwise temperature gradient. It became clear that for polypeptides with molecular weights of approximately 3,000, by simply controlling the hydrophobic interaction we were able to realize separation in an aqueous environment.[11)] Considering how important it is to be able to maintain biological activity and a high survival rate after separation — especially when separating protein and cells — as with this method separation can be carried out only in a water-based eluent it would be highly suitable as it satisfies those conditions. The column packed with octadecyl silica beads are widely used for separation in a mixture eluent of water and organic solvents and recognized as one of the powerful tool for analyses. However, the reversed-phase chromatography cannot be utilized for separation of proteins and cells. Therefore, it became clear that the newly developed thermoresponsive columns could be used in place of the reversed-phase chromatography for carrying out separation.

By introducing weak acid or base groups to the thermoresponsive polymers as the column matrix modifiers, bioactive molecules with charged, and hydrophobic characteristics, can be separated.[13),14)] Angiotensin peptides consist of three subtypes having similar molecular weights but distinct biological activities, and are conventionally separated by combining a number of stages of